Rapid Profiling of Disease Alleles Using a Tunable Reporter of Protein Misfolding

Adrianne M. C. Pittman,* Melissa D. Lage,* Vladimir Poltoratsky,* Justin D. Vrana,† Alessandro Paiardini,‡ Alessandro Roncador,§ Barbara Cellini,§ Robert M. Hughes,* and Chandra L. Tucker*,†,1

*Department of Biology, Duke University, Durham, North Carolina 27708, †Department of Pharmacology, University of Colorado Denver School of Medicine, Aurora, Colorado 80045, ‡Department of Biochemical Sciences, "Sapienza" University of Rome, 00185 Rome, Italy, §Department of Life Sciences and Reproduction, Section of Biological Chemistry, University of Verona, 37134 Verona, Italy

ABSTRACT Many human diseases are caused by genetic mutations that decrease protein stability. Such mutations may not specifically affect an active site, but can alter protein folding, abundance, or localization. Here we describe a high-throughput cell-based stability assay, IDESA (intra-DHFR enzyme stability assay), where stability is coupled to cell proliferation in the model yeast, *Saccharomyces cerevisiae*. The assay requires no prior knowledge of a protein's structure or activity, allowing the assessment of stability of proteins that have unknown or difficult to characterize activities, and we demonstrate use with a range of disease-relevant targets, including human alanine:glyoxylate aminotransferase (AGT), superoxide dismutase (SOD-1), DJ-1, p53, and SMN1. The assay can be carried out on hundreds of disease alleles in parallel or used to identify stabilizing small molecules (pharmacological chaperones) for unstable alleles. As demonstration of the general utility of this assay, we analyze stability of disease alleles of AGT, deficiency of which results in the kidney stone disease, primary hyperoxaluria type I, identifying mutations that specifically affect the protein-active site chemistry.

GENETIC mutations that reduce protein stability are common causes of human disease. Many disease proteins are difficult to characterize or have unknown activities, and understanding the consequences of a particular mutation, and its effects on activity and stability, can be correspondingly difficult. Destabilized proteins often retain the ability to function at a low level, but as a result of instability may be degraded by the cell's quality control machinery or localized to an incorrect cellular compartment (Cheng *et al.* 1990; Purdue *et al.* 1990). For proteins that are partially functional, addition of stabilizing molecules, such as compounds that directly bind to the protein or stimulate chaperones, may help to alleviate the disease phenotype (Lumb *et al.* 2003; Yam *et al.* 2005).

High-throughput cell-based screens have been productive in identifying compounds that rescue misfolded proteins (Pedemonte *et al.* 2005; Cooper *et al.* 2006; Ehrnhoefer *et al.* 2006; Mu *et al.* 2008; Neef *et al.* 2010; Su *et al.* 2010), but these screens are typically designed for a specific protein activity and not generalizable for use with other proteins. A variety of generalizable approaches to analyzing protein stability are available *in vitro*, but these approaches require purified protein and do not allow assessment of protein stability within the cellular environment. *In vivo*, the most common general approaches to examine protein stability are Western blot or pulse-chase analysis, which allow proteins to be studied in the cellular milieu, but such analysis is not amenable to high-throughput studies.

In the past few years, several *in vivo* stability reporters have been developed, including fusion with GFP (Waldo *et al.* 1999), complementation of β-galactosidase (Wigley *et al.* 2001), and split versions of GFP (Cabantous *et al.* 2008) and β-lactamase (Foit *et al.* 2009). The latter two reporters used an insertional approach, where a target protein was inserted directly into a reporter, reducing false positives due to proteolysis or initiation of protein translation at internal sites, which can untether the reporter from the target protein (Cabantous *et al.* 2008). Using a similar insertional approach, we present here a novel stability assay, IDESA (intra-

doi: 10.1534/genetics.112.143750
Manuscript received July 11, 2012; accepted for publication August 10, 2012
[1]Corresponding author: Department of Pharmacology, MS 8303, Box 6511, University of Colorado—Denver, School of Medicine, Aurora, CO 80045. E-mail: chandra.tucker@ucdenver.edu

dihydrofolate reductase [DHFR] enzyme stability assay), that is designed for high-throughput use in eukaryotic cells.

In this report, we demonstrate use of IDESA to report subtle changes in steady-state protein levels in cells that relate to stability differences. Importantly, we show that the assay can be fine tuned with individual target proteins to increase the dynamic range of the reporter, allowing subtle changes in stability to manifest as robust changes in growth. Using a variety of human disease related proteins—superoxide dismutase, SOD-1 (associated with familial amyotrophic lateral sclerosis, ALS), DJ-1 (associated with Parkinson's disease), SMN1 (associated with spinal muscular atrophy (SMA)), p53 (associated with cancer), and alanine:glyoxylate aminotransferase (AGT, associated with primary hyperoxaluria type I, PH1)—we show that the assay is tunable such that strong growth differences can be observed between wild-type and mutant proteins. Our studies demonstrate that IDESA provides a powerful and facile approach for high-throughput characterization of protein stability *in vivo*.

Materials and Methods

Strains and plasmids

Yeast strains *W303-1A (MAT***a** *ade3-1 can1-100 ura3-1 leu2-3,112 his3-11,15 trp1-1)*, *TH5 (MAT***a** *leu2-3,112 trp1 ura3-52 dfr1*::*URA3 tup1)*, *TH5*Δ*pdr5 (MAT***a** *leu2-3,112 trp1 ura3-52 dfr1*::*URA3 tup1 pdr5*::*KanMX)*, and *PJ69-4a (MAT***a** *trp1-901 leu2-3,112 ura3-52 his3-200* Δ*gal4* Δ*gal80 LYS2*::*GAL1-HIS3 GAL2-ADE2 met2*::*GAL7-lacZ)* were used. Human *cDNAs* for *SOD-1* and *DJ-1* were obtained from Open Biosystems.

The DHFR fusion constructs were generated in plasmid pTB3–dhfr, which contains 600 bp of the *Saccharomyces cerevisiae DFR1* promoter-controlling expression of a mouse DHFR protein split with a linker at residue 107. To generate specific insertions within DHFR, pTB3–dhFK or pTB3–P66LdhFK (Tucker and Fields 2001) were digested with *Nhe*I and *Cla*I to remove an inserted FKBP12 protein, and target protein open reading frames were inserted between these sites, flanking amino acid 107 and amino acid 108 of mouse DHFR, using homologous recombination in yeast. Disease mutations were generated by PCR and cloned into pTB3 (or pTB3–P66L) using homologous recombination. To generate methotrexate resistant (MTX^r) DHFR variants, the L22F/F31S amino acid substitutions in DHFR were introduced into pTB3–dhAGT by PCR and integrated using homologous recombination in yeast. Generation of HA-tagged AGT variants used in half-life studies (Figure 2E) is described previously (Hopper *et al.* 2008). To generate pESCLeu–dhAGT constructs used in Figure 3B, the dhfrN-AGT-dhfrC (dhAGT) fusions were excised from pTB3 using *Bam*HI and *Xba*I and cloned into the plasmid pESCLeu (Agilent Technologies) using *Bam*HI and *Sal*GI sites. To generate HA-tagged pESCUra–MTX^r-dhAGTmi (Figure 3A), a HA tag was introduced at the C terminus of MTX^r-dhAGTmi via PCR, and this fragment was cloned via ligation into pESCUra (Agilent Technologies) digested with *Bam*HI and *Hin*dIII. The DHFR C-terminal fusions used in Figure 3C were generated by overlap extension PCR and cloned via homologous recombination into pTB3 cut with *Bam*HI and *Eco*RI, downstream of the DHFR promoter on pTB3. To generate HA-tagged pP66LdhSOD^{G37R} (Figure 6), the P66LdhSOD^{G37R} insert from pTB3 was cut at *Bam*HI and *Eco*NI sites and ligated into a p414GalL–dhERa-HA construct (containing a HA-tagged estrogen receptor ligand binding domain inserted in DHFR (Tucker and Fields 2001)), also cut with *Bam*HI and *Eco*NI.

Growth assays

For assays carried out using strain TH5, yeast were grown to log phase in SD–Trp media supplemented with 100 μg/ml dTMP (Sigma), which allows survival of *dfr1* yeast. Cells were washed in water, diluted to 0.05 OD_{600} in SD–Trp media lacking dTMP, and grown for indicated periods of time. Growth was quantified by measuring the turbidity of the yeast cultures at OD_{600} using a SpectraMax 190 plate reader (Molecular Devices). For growth assays carried out using methotrexate in W303-1A cells, cells were grown to log phase in SD–Trp media, then diluted to an OD_{600} of 0.05 in SD–Trp media with 80 μM methotrexate and grown for specified periods of time. For growth assays using PCB/light induction, pESCUra–MTX^r-dhAGTmi was transformed into strain PJ69-4a along with PhyB(NT)–GBD and PIF3–GAD (Shimizu-Sato *et al.* 2002), and cells were grown overnight in SD–Trp/–Leu/–Ura media. The next morning, cells were diluted to an OD_{600} of 0.05 in the same media, and then 80 μM methotrexate and indicated amounts of phycocyanobilin (PCB) were added. Cells were exposed to a 1-min flash of red light (660 nm) using an LED light source every 2 hr during the growth assay. PCB was extracted by methanolysis from Spirulina.

Western blotting

Galactose-inducible constructs expressed in W303-1A were grown overnight in SD–Leu media, diluted to an OD_{600} of 0.2, then grown to log phase in SD–Leu containing 2% raffinose. At OD_{600} ~0.6, galactose was added to a final concentration of 2% and cells were incubated for 4 hr at 30°. Yeast were lysed with glass beads in 200 μl PBS containing 1 mM PMSF and protease inhibitors (Complete Mini EDTA-free, Roche). Lysates were centrifuged at 14,000 rpm for 10 min, and an equal volume of 2× LSB was added to the supernatants before storage. For experiments using PCB, cultures were induced as described for growth assays with PCB but grown without methotrexate. Cells were grown a total of 20 hr and lysed as described with W303-1A cells. Equal amounts of total protein were run on an SDS–PAGE gel and immunoblotted using standard procedures using a rabbit α-AGT primary antibody (a gift from Chris Danpure, UCL) and an IRDye 800CW goat anti-rabbit IgG secondary antibody (Li-COR) for experiments shown in Figure 2B or a mouse anti-HA (monoclonal) primary antibody (Covance)

and an IRDye 700CW goat anti-mouse IgG secondary (Li-COR) for experiments shown in Figure 3A and Figure 6B. Proteins were visualized using an Odyssey infrared imaging system (Li-COR).

Thermostability studies

The thermostability of the F152I-Mi variant in the holo- (in the presence of 10 μM exogenous pyridoxal 5′-phosphate, PLP) and apo-form at 10 μM concentration was determined by monitoring the loss of the CD signal at 222 nm with temperature increasing from 25° to 90° at a heating rate of 1.5°/min. The T_m values were calculated by fitting the data to a two- or a three-state unfolding model using the Origin Pro7 software according to the method of Pace *et al.* (1989). The protein was expressed in *Escherichea coli* and purified as previously described (Cellini *et al.* 2007, 2008).

Half-life determination

HA-tagged AGT variants in p416GPD were expressed in strain W303-1A and grown to log phase (OD_{600} ~0.8). Cycloheximide was added to 35 μg/ml and cells were lysed at 0, 30, and 110 min after cycloheximide addition. Lysis was carried out by vortexing with glass beads in lysis buffer (25 mM Tris pH 6.8, 150 mM NaCl, 1% SDS, 10 mM EDTA, 5 mM PMSF, and protease inhibitors [1×, Complete Mini EDTA-free, Roche]) at 4° for 1-min intervals (repeated six times). Cell debris was removed by centrifugation, and the supernatant was mixed with 4× LSB and loaded on an SDS–PAGE gel for immunoblotting. Immunoblotting was carried out using standard procedures using a mouse anti-HA (monoclonal) primary antibody (Covance) and a HRP-conjugated goat anti-mouse IgG secondary (Santa Cruz Biotechnology). Half-lives were calculated as in Belle *et al.* (2006), where the ln(intensity) *vs.* time was plotted and fit to a first-order decay function to determine the degradation rate constant k, and then the half-life was calculated from the equation $T_{1/2} = \ln(2)/k$.

Molecular dynamics

The crystal structure coordinates of human AGT from Brookhaven Protein Data Bank (PDB) (Sussman *et al.* 1998) were used as a starting structure for molecular dynamics (MD) simulations of AGTmi, AGTmi^{S275R}, and AGTmi^{E274D}. For each simulation, the crystal structure was checked and missing residues (residues: 1–3; 121–122; 392) and amino acid substitutions for AGTmi^{S275R} and AGTmi^{E274D} were modeled using Modeler 9v5 (Sali and Blundell 1993). Since the dimeric crystal structure was obtained in the presence of two cofactor PLP moieties, the Amber 10 forcefield and the auxiliary Antechamber tool were adopted to recognize the atom and bond type of the system, generate residue topology files, and find missing force field parameters. The resulting structure was energy minimized in vacuum, using the Amber 10 forcefield and Gromacs 3.3.3 package (Van Der Spoel *et al.* 2005). After an initial minimization performed to allow added hydrogens to adjust to the crystallographically defined environment, a 5000-step steepest descent minimization without periodic boundary conditions was performed, until the maximum derivative was <0.01 kJ/Mol/Å. Then, the system was soaked by a water box of 97 × 97 × 97 Å^3 dimensions, filled with a total of 20142 water molecules, and counterions were added to neutralize the net negative charge of the protein and obtain a concentration of 0.01 M Na^+/Cl^-. Energy minimization was then performed for 5000-steps steepest descent, but this time periodic boundary conditions were introduced. Then, keeping the nonhydrogen atoms of the proteins fixed to the reference positions, a position-restrained MD was performed for 10 picoseconds (ps) at −223° (50K), to let the solvent adapt to the protein. After pressure coupling, the system was gradually heated at 25° (298K) during 50 ps simulation at temperature increments of −223° (50K) every 10 ps. Finally, a production simulation was carried out for 3 nanoseconds, with a time step for integration of 0.2 femtoseconds. Bond lengths were constrained by using the Linear Constraint Solver (LINCS) algorithm.

Chemical screens

For chemical screening, the strain TH5Δ*pdr5* was used to increase the permeability of small-molecule compounds. Yeast expressing P66L-dhDJ1^{L166P} were grown to log phase in SD–Trp media supplemented with 100 μg/ml dTMP (Sigma). Cells were washed in water, diluted to 0.05 OD_{600} in SD–Trp media lacking dTMP, and then aliquoted into 96-well plates. Chemicals (Sigma LOPAC) were added at a final concentration of 20 μM using a Biomek FX robotic device (Beckman). Plates were incubated for 3 days, and the OD_{600} for each well was measured using a plate reader. Screens were carried out in duplicate, and samples showing growth that was >2 SD from the plate mean in duplicate screens were considered hits. Hits from the screen were confirmed by individual titration assays in the TH5 strain using compounds purchased from Sigma.

Results

Analysis of disease variants using IDESA

The IDESA platform is based on a prior developed yeast ligand sensor (Tucker and Fields 2001), in which a DHFR fusion protein complements growth of a yeast strain lacking DHFR. A target protein of interest is inserted internally in DHFR, thus closely linking stability of the target protein with that of DHFR. A weak promoter (yeast *DFR1*) is used to express low levels of the DHFR fusion protein. Growth of yeast is linked to DHFR activity and protein levels, such that mutations that reduce stability would be expected to decrease the amount of functional DHFR activity, and thus decrease growth of yeast.

To first test the ability of IDESA to accurately monitor protein stability, we used the enzyme AGT. Missense

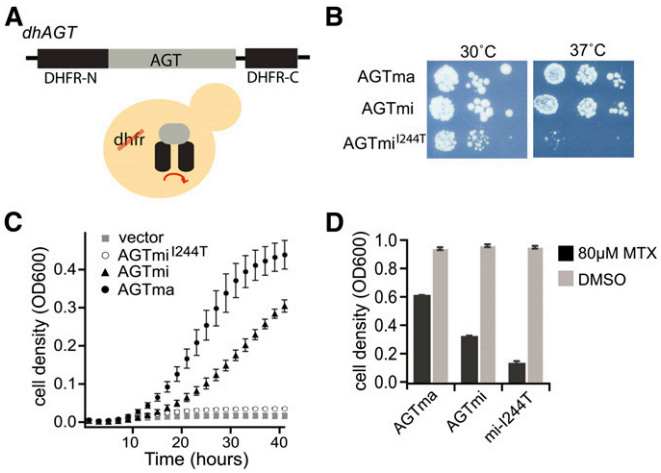

Figure 1 Use of IDESA stability assay with AGT variants. (A) Schematic showing IDESA construct. The AGT protein was inserted at amino acid 107 of DHFR, and this construct was expressed in yeast cells lacking DHFR. (B) TH5 yeast expressing indicated dhAGT constructs were spotted in 10-fold serial dilutions and incubated at indicated temperatures for 3 days. (C) Growth of pTB3–dhAGT variants expressed in TH5 cells at 37° was monitored in 96-well plates for 40 hr. The vector control contained p414ADH. (D) Growth of W303-1A strains expressing methotrexate resistant dhAGT variants (pTB3–MTX^r-dhAGT) in the presence of 80 μM methotrexate or with DMSO carrier. Samples were incubated for 21 hr at 37° in 96-well plates. The data represent the average and standard deviation (SD) for three independent wells.

mutations of AGT cause PH1, a severe autosomal recessive kidney stone disease (Danpure and Jennings 1986). We inserted the wild-type (major allele) human AGT protein into mouse DHFR to generate a fusion protein, dhAGTma (Figure 1A). This fusion protein was expressed in a TH5 strain lacking the yeast DHFR gene *dfr1* (Tucker and Fields 2001), where we observed complementation of the *dfr1* deficiency (Figure 1, B and C). We next analyzed alleles of AGT associated with PH1, including a minor allele polymorphic variant (AGTmi, with amino acid substitutions P11L and I340M), and a disease variant associated with the minor allele, I244T (AGTmi^{I244T}). AGTmi has a mild destabilizing effect, while the AGTmi^{I244T} disease variant has greatly reduced stability (Lumb and Danpure 2000; Hopper *et al.* 2008; Cellini *et al.* 2010a). Using IDESA, we observed robust differences in growth of yeast expressing these variants, with yeast expressing AGTmi and AGTmi^{I244T} showing poorer growth than yeast expressing wild-type AGT and yeast expressing AGTmi^{I244T} showing a temperature-sensitive phenotype at 37° (Figure 1, B and C).

IDESA uses a DHFR reporter, requiring that the strain used for growth have a nonfunctional yeast DHFR protein. To broaden the applicability of IDESA for use in other yeast strains or mammalian cell lines that might contain a functional DHFR, we tested a modified version of this assay. We introduced L22F and F31S mutations in DHFR that cause resistance to methotrexate, a DHFR inhibitor (Ercikan-Abali *et al.* 1996; Tarassov *et al.* 2008). These mutations do not affect DHFR activity (Ercikan-Abali *et al.* 1996), but allow growth to be assayed in the presence of methotrexate, which inhibits the endogenous yeast DHFR enzyme but not the resistant DHFR fusion. Using this approach, we examined growth of yeast expressing the same dhAGT variants described above. A MTX^r L22F/F31S version of DHFR was expressed in a *DFR1*$^+$ strain, W303-1A, in the presence or absence of 80 μM methotrexate (Figure 1D). This concentration of methotrexate sufficiently inhibited yeast Dfr1 activity, resulting in growth that was dependent on activity of the dhAGT fusion protein and that was comparable to growth in the TH5 strain (Figure 1D). Thus, using methotrexate resistance mutations, this assay can be extended for use in any yeast strain or even mammalian cell lines containing DHFR.

Relationship between protein stability and growth

We hypothesized that the reduced growth of yeast in IDESA seen with disease alleles could reflect either reduced steady-state levels of protein or reduced DHFR activity (*i.e.*, the two halves of DHFR may not form an active enzyme as easily when separated by a less stable protein). To distinguish between these, we compared the growth of yeast expressing different AGT alleles with measurements of their cellular steady-state levels. In addition to AGTmi^{I244T}, we examined two other disease alleles associated with the minor allele, AGTmi^{G170R} and AGTmi^{F152I}. These alleles have reduced stability, resulting in increased aggregation *in vitro* and mislocalization *in vivo* (Lumb and Danpure 2000). Similar to AGTmi^{I244T}, growth of yeast expressing AGTmi^{G170R} or AGTmi^{F152I} was greatly reduced (Figure 2A). In all cases tested, the reduced growth correlated with reduced steady-state levels of protein (Figure 2B), which could be represented by a linear relationship (Figure 2C).

To more rigorously explore the relationship between protein stability and yeast growth, we compared the thermodynamic stabilities of AGT variants with their growth rates in IDESA. Previous studies have demonstrated a strong link between thermodynamic protein stability and the stability of a protein in a cell (Parsell and Sauer 1989). We compared the growth of yeast expressing mutant forms of AGT with their *in vitro* melting temperatures calculated in the holo- (bound to a PLP cofactor) or apo-forms, shown in Table 1. Previous work has shown that the apo-form of AGT unfolds in two steps indicative of two domains, which can be represented by two melting temperatures, T_{m1} and T_{m2} (Oppici *et al.* 2012). Several mutant AGT variants show no defect in T_{m1} , but do not undergo a T_{m2} transition, indicative of a molecular defect confined to the second domain (Oppici *et al.* 2012). In addition to alleles analyzed in Figure 1, we examined S158L-ma, W108R-mi, G350D-mi, and G161S-mi. The mutations S158L and W108R are in residues that contact the PLP cofactor in the active site of the enzyme (Zhang *et al.* 2003), and these mutants show significantly reduced catalytic activity and reduced affinity for PLP (Oppici *et al.* 2012). The G161S mutation is in a region bridging the two domains of AGT, and both holo- and apo-forms are destabilized. G350D, in a random coil region

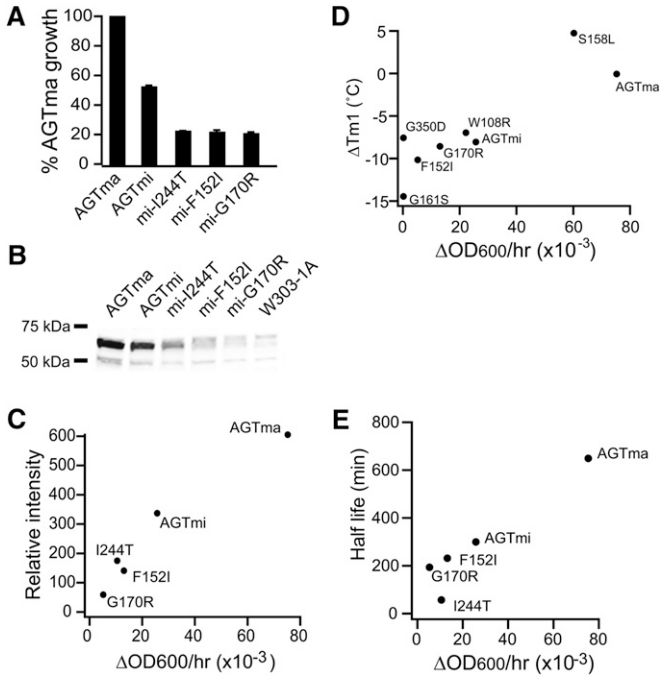

Figure 2 IDESA reports changes in protein steady-state levels that correlate with thermodynamic protein stability. (A) Growth of W303-1A strains expressing methotrexate resistant dhAGT variants (pTB3–MTX^r-dhAGT) in the presence of 80 μM methotrexate. Samples were incubated for 21 hr at 37° in 96-well plates. Growth is expressed as a percentage of wild-type AGTma growth. The data represent the average and SD for three independent wells. (B) Immunoblot analysis of pESCLeu–dhAGT variants expressed in strain W303-1A. The sample labeled W303-1A represents cells alone. (C) Graph comparing growth of AGT variants in IDESA (pTB3–MTX^r-dhAGT in W3031A) on the *x*-axis with relative intensity of Western blot bands shown in B. (D) Graph comparing growth of AGT variants in IDESA (pTB3–MTX^r-dhAGT in W3031A) with ΔT_{m1} of the apo form of the purified protein (relative to T_{m1} of AGTma), where ΔT_{m1} = apo $T_{m1}{}^{AGTma}$– apo $T_{m1}{}^{mutant}$. (E) Graph comparing growth of AGT variants (as in C and D) with determined half-lives of the HA-tagged variants expressed in yeast strain W303-1A.

near the active site, has been proposed to specifically affect the structure of the second domain, as measured by a loss of T_{m2} (Oppici *et al.* 2012).

In general, we found that T_{m1} of the apo-protein showed the strongest correlation with growth (Figure 2D). Most, but not all, of the proteins that grew poorly in IDESA also showed a corresponding reduction in stability *in vitro* as measured by T_{m1}. One exception was G350D-mi, which grew poorly in IDESA but showed normal stability as measured by T_{m1} (Figure 2D). However, as mentioned previously, the structural defect of this protein appears to be confined to the second domain monitored by T_{m2}. The variant G170R-mi also showed reduced growth in IDESA but shows equivalent stability as AGTmi *in vitro*. This variant is highly aggregation prone (Coulter-Mackie and Lian 2006), a property that would not be revealed by the melting curve studies on purified proteins but that would affect its stability within cells.

As thermodynamic stability is a key determinant, but not the sole determinant, of *in vivo* protein stability, we also

Table 1 Stability of purified AGT variants

Variant	T_{m1} holo	T_{m1} apo	T_{m2} apo
AGTma	77.5	61.1	66.4
AGTmi	73.6	53.1	66
G170R-mi	72.2	52.6	64.9
F152I-mi	72	51	67
W108R-mi	54.1	54.2	
G350D-mi	73.5	53.6	
G161S-mi	62.5	46.7	
S158L-ma	67	64.3	

Stability data obtained from Oppici *et al.* (2012) or this article.

examined stability differences by monitoring protein half-lives in the cell via cycloheximide chase (Belle *et al.* 2006). Protein synthesis of HA-tagged versions of AGTma, AGTmi, or mutant constructs was halted with cycloheximide, and aliquots were taken for immunoblot analysis at 0, 30, and 110 min after cycloheximide addition. As shown in Figure 2E, we also observed a linear correlation between protein half-life and growth in IDESA, with mutant proteins with reduced *in vivo* half-lives showing poorer growth in IDESA.

Analysis of IDESA sensitivity and reproducibility

We carried out additional experiments to examine the sensitivity and reproducibility of IDESA. To examine the sensitivity of IDESA to different protein levels, we used an inducible system to express increasing amounts of MTX^r dhAGTmi. The inducible system, which uses light and a small molecule PCB to induce transcription (Shimizu-Sato *et al.* 2002), allowed us to generate precise levels of expressed MTX^r dhAGTmi (Figure 3A). Subtle increases in protein levels corresponded to precise cell growth increases, providing further demonstration of the sensitivity of the growth assay to detect small changes in protein levels (Figure 3B).

To test the reproducibility of IDESA, we examined growth of strains expressing dhAGTma and AGTmi^{I244T} in six independent assays. In parallel, we also examined the same variants using a reporter consisting of DHFR fused to the C terminus of AGT (AGT–DHFR). In previous studies, N-terminal or C-terminal-fused reporters of protein stability have presented problems when used *in vivo*, as their stabilities can become uncoupled from the stabilities of the proteins they are monitoring (Cabantous *et al.* 2008). In these cases, both proteolytic cleavage and internal translation initiation can separate the reporter from its target, giving rise to variable growth within cells (Cabantous *et al.* 2008). Yeast expressing AGT–DHFR fusions indeed showed variable growth with multiple experiments (Figure 3C). In contrast, strains expressing IDESA constructs (containing the target protein inserted within DHFR) gave consistent results in independent experiments (Figure 3D). Thus IDESA, like other inserted reporters, provides a stable platform for studies, likely due to a reduction in events that would untether the reporter from the target protein.

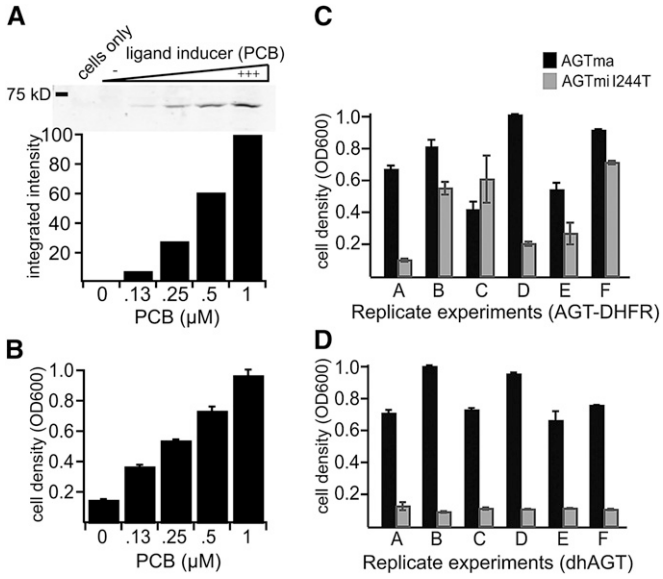

Figure 3 Sensitivity and reproducibility of IDESA. (A and B) Examination of sensitivity of IDESA, using a PCB-inducible system to express precise amounts of dhAGTmi protein. Yeast strain PJ69-4a was transformed with pESCUra–MTX^{r}-dhAGTmi, as well as PhyB(NT)–GBD and PIF3–GAD, which allow red light and ligand (PCB)-dependent transcriptional induction of Gal4-regulated genes. (A) Yeast were grown for 20 hr at 30° in the presence of indicated amounts of PCB, and levels of HA-tagged dhAGTmi were quantified by immunoblot. The relative quantitation of the immunoblot bands (arbitrary units) is shown below. (B) The same yeast as in A were placed in media containing 80 μM methotrexate and indicated amounts of PCB and assayed for growth after 20 hr. Error bars, SD. (C and D) Examination of reproducibility of IDESA. Yeast expressing wild-type AGT or AGTmi^{I244T} were fused to an intact C-terminal mouse DHFR protein (AGT–DHFR and AGTmi^{I244T}–DHFR) (C), or inserted within DHFR via the IDESA assay (in pTB3–dhAGT) (D). Growth of TH5 cells expressing each construct was independently assessed 6 times (samples A–F indicated on the *x*-axis) after 38–42 hr. Growth was monitored in 96-well plates. Error bars, SD.

Characterization of uncharacterized disease alleles of AGT

To further explore the utility of IDESA for characterization of disease alleles, we examined uncharacterized disease alleles from PH1 patients to determine effects on AGT protein stability. The mutation S205P is predicted to alter the protein's central β-sheet and significantly destabilize AGT (Zhang *et al.* 2003). In agreement with this prediction, we found that yeast expressing AGT^{S205P} were unable to grow, indicating severe instability (Figure 4A). We next examined two mutations (R289C, L298P) found in a homozygous form on both alleles (on the minor allele background) in a single PH1 patient (Frishberg *et al.* 2005). AGTmi^{R289C} showed equivalent stability as AGTmi, but stability of AGTmi^{L298P} was greatly impaired, providing strong evidence that the L298P mutation alone is responsible for the disease in this patient (Figure 4A). A number of pathogenic AGT mutations cause disease only in combination with the minor allele, and we examined whether IDESA could discriminate between these mutations. Mutations G161R and C253R were analyzed in combination with either the major (wild-type) allele or minor allele using IDESA (Figure 4A). While C253R had little effect on stability of the major allele protein, this mutation significantly destabilized the minor allele protein. In contrast, G161R destabilized both alleles. In agreement with these results, the G161R mutation has been described in a patient on the major allele, while C253R has been found to cause disease only in combination with the minor allele (Williams *et al.* 2009).

We next used IDESA to examine a larger set of disease-related variants. We were interested in whether IDESA could discriminate between loss-of-function mutations, allowing us to identify mutants that specifically perturb functionality but do not result in large-scale structural changes. For proteins with unknown or undefined functions, identification of disease variants that affect activity but not stability can provide clues to their mechanisms of action. We chose 35 disease variants of AGT from PH1 patients (Williams *et al.* 2009) that showed loss of function (<10% of wild-type AGT activity) in a yeast activity assay based on complementation (Hopper *et al.* 2008). Within this set, we identified 12 mutants that showed good stability in IDESA (Figure 4B, top), but poor activity in the complementation assay (Figure 4B, bottom). Of these, four (G82R, H83R, W108R, and S158L) contained mutations in residues that coordinate the PLP cofactor in the active site of the enzyme (Zhang *et al.* 2003). Also in this group was H261Q, adjacent to Tyr260, another residue involved in coordinating PLP. G41E and G41R, located at the dimerization interface of AGT, were included in this group. G41R has been characterized in depth *in vitro*, where it has been shown to affect dimerization, reduce affinity of AGT for PLP (Cellini *et al.* 2010b), and significantly increase aggregation under physiological conditions. Molecular dynamics simulations of this mutant revealed unwinding of the 34–42 α-helix and displacement of the first 44 amino acid residues, including an active site loop at residues 24–32 (Cellini *et al.* 2010b). While not involved in coordinating PLP, Gly47 is also near the active site of the enzyme, and the replacement of the smaller glycine in the G47R variant may locally perturb the structure.

While most of the variants identified in this group had mutations in or near the protein active site, three variants (AGTmi^{R36C}, AGTmi^{E274D}, and AGTmi^{S275R}) contained mutations at residues distal from the active site (Figure 4C). These three residues cluster in the tertiary structure of the enzyme: Glu274 and Ser275 are on adjacent residues of α-helix 266–282, located opposite from Arg36 in α-helix 34–42 on the same monomer (Figure 4C). Using molecular dynamics simulation studies, we examined the effects of the E274D and S275R substitutions (Figure 4D). While AGTmi^{E274D} showed no difference from AGTmi in simulations, the replacement of Ser for the bulkier Arg in S275R was found to displace Leu211 and Ser207, resulting in a partial distortion of active site loop 206–216 (Figure 4D). As this loop contains Lys209, the residue that covalently binds PLP

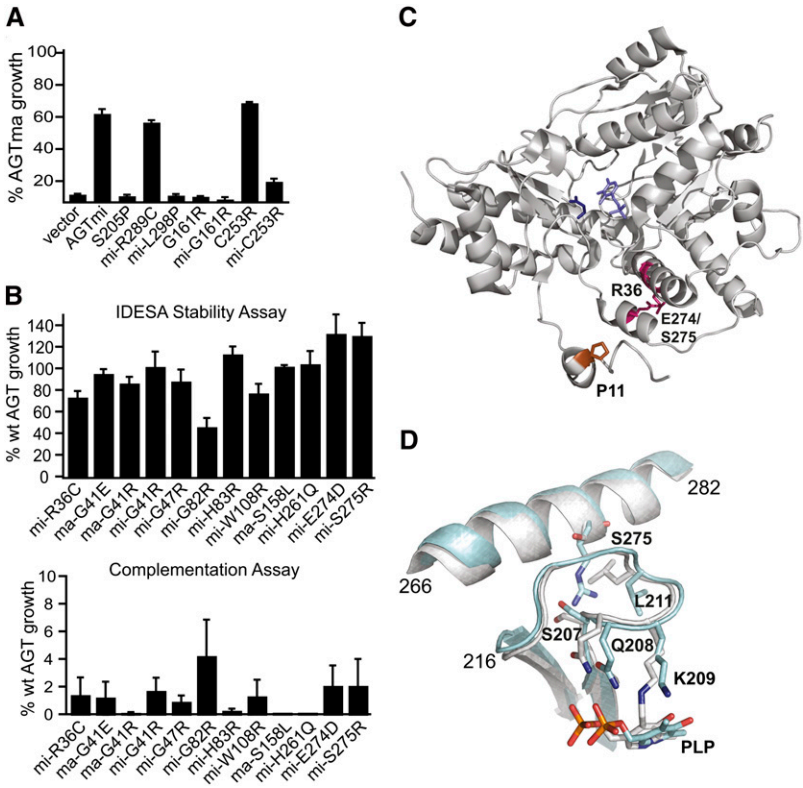

Figure 4 Analysis of pathogenic disease alleles of AGT using IDESA. (A) Growth of PH1-associated AGT mutant proteins in IDESA. Growth is expressed as a percentage of wild-type AGTma growth. Mutants on the minor allele (AGTmi) background are indicated by "mi." Error bars, SD. (B) A subset of pathogenic AGT mutant proteins show near wild-type stability in IDESA (top) but have <5% of wild-type activity as measured by a complementation assay in yeast (bottom). Each mutant was generated in the major (ma) or minor (mi) allele background as indicated, and growth of each mutant is expressed as a percentage of wild-type growth (AGTma or AGTmi, depending on the allele background). Error bars, SEM. (C) Location of R36, S275, and E274 on adjacent helices of the AGTma monomer. Pro11, which is changed to Leu in AGTmi, is also indicated in the structure. (D) Molecular dynamics simulations of AGTmi^{S275R}. The AGTmi structure is shown in gray. Rearrangements caused by the substitution of Arg at residue 275 are shown in blue.

via formation of a Schiff base, this substitution may alter PLP binding in the active site. We are currently examining these mutants *in vitro* in greater detail to better understand how they may specifically perturb the protein active site chemistry.

Tunability of IDESA with a variety of protein targets

To determine whether IDESA is generalizable to a broad range of protein targets, we examined the growth of yeast expressing wild-type and mutant forms of four additional human disease-related proteins, DJ-1, SOD-1, SMN1, and p53 associated (respectively) with familial ALS, Parkinson's disease, SMA, and cancer. With SOD-1, we examined three disease variants (A4V, G37R, and G85R), which were previously shown to have reduced stability (Cardoso *et al.* 2002; Stathopulos *et al.* 2003; Furukawa and O'halloran 2005; Lindberg *et al.* 2005; Shaw and Valentine 2007). The A4V mutation, which affects the dimer interface of SOD-1, is particularly severe and has been shown to result in significant destabilization *in vitro* and rapid aggregation (Cardoso *et al.* 2002; Leinweber *et al.* 2004). Yeast expressing this variant showed temperature-sensitive growth even at 30° (data not shown), while yeast expressing wild-type SOD (dhSOD), dhSOD^{G37R}, and dhSOD^{G85R} demonstrated indistinguishable growth at 30° (Figure 5). As increasing the temperature places stress on the cell and can uncover temperature-sensitive phenotypes, we tested SOD-1 variants at temperatures up to 39°. SOD-1 is an unusually stable protein (Forman and Fridovich 1973), and we were unable to identify a difference in growth between yeast expressing wild-type dhSOD, dhSOD^{G37R}, or dhSOD^{G85R} even at higher temperatures. To allow observation of growth differences at lower temperatures, we added a destabilizing mutation (P66L) to DHFR (Dohmen *et al.* 1994; Tucker and Fields 2001), which we speculated would act additively with the disease mutations. Addition of this mutation to dhSOD caused a large reduction in growth rate, allowing clear discrimination between wild-type and disease forms of SOD-1 at 30° and resulting in temperature-sensitive growth of the mutant proteins but not wild-type at 37° (Figure 5).

We used the same approach to examine three mutant forms of human DJ-1: L166P, M26I, and D149A. The L166P mutation disrupts dimer formation and greatly reduces stability *in vitro* and *in vivo* (Blackinton *et al.* 2005; Malgieri and Eliezer 2008). The M26I and D149A mutations appear milder than L166P, with M26I showing ~50% reduced expression in cell culture and decreased dimerization and stability *in vitro* (Blackinton *et al.* 2005; Malgieri and Eliezer 2008). The D149A mutant appears the mildest, showing decreased stability *in vitro* but normal dimerization and only slightly reduced levels in cultured cells (Blackinton *et al.* 2005; Malgieri and Eliezer 2008). Yeast expressing wild-type DJ-1 inserted in DHFR (dhDJ1) grew similar to yeast expressing mutant forms at 30°, while at 37°, dhDJ1^{M26I} and dhDJ1^{L166P} showed a slight reduction in growth (~61–69% of wild-type at 48 hr) (Figure 5). As with SOD-1, addition of a destabilizing P66L mutation in DHFR reduced growth, such that at 30° the disease mutants showed clearly reduced growth compared to wild type. In agreement with previous studies, M26I and L166P had more severe effects than D149A.

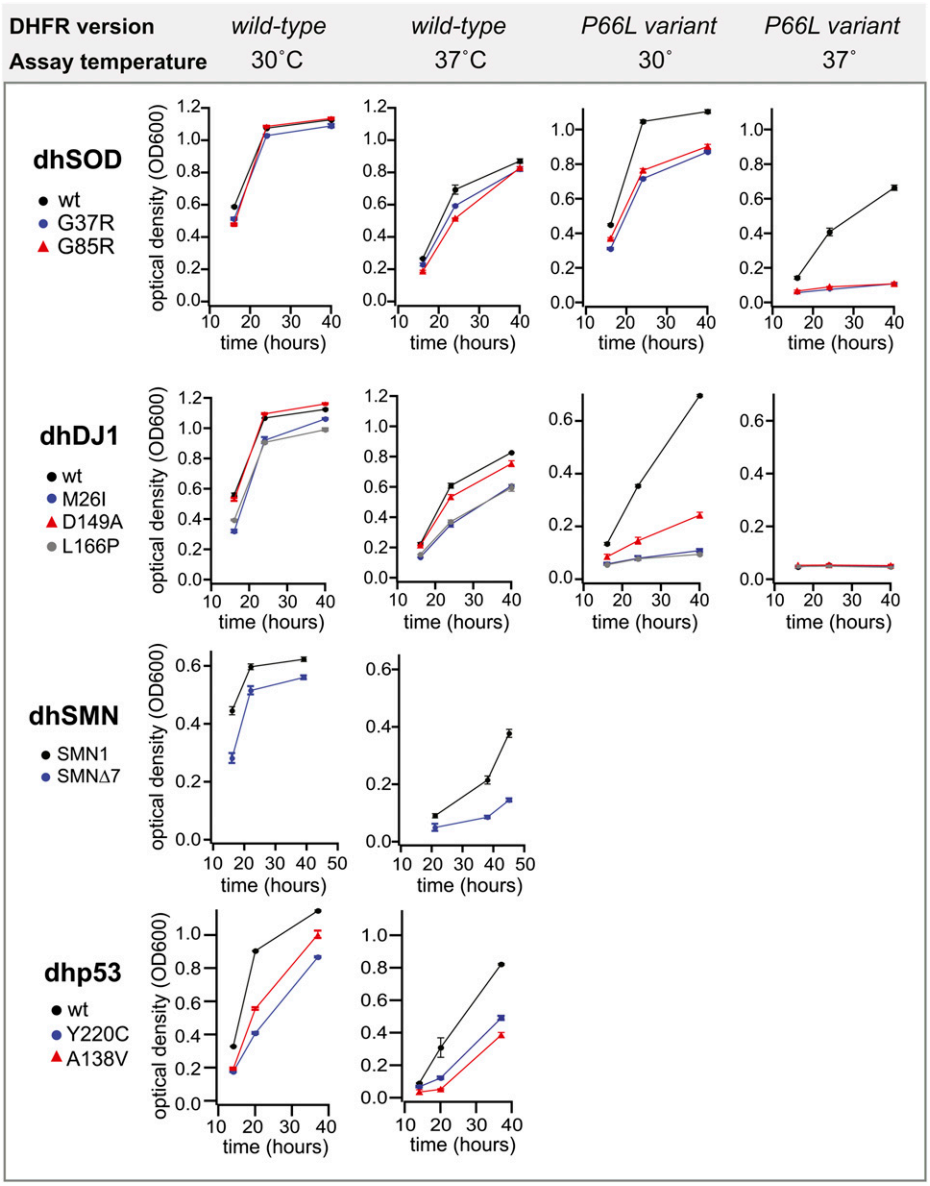

Figure 5 Temperature and destabilizing mutations allow tuning of IDESA. Wild-type or mutant versions of SOD1 (dhSOD), DJ-1 (dhDJ1), SMN1 (dhSMN), or p53 (dhp53) were tested using IDESA. Mutants tested are indicated in the legend at left. Assays were carried out in TH5 cells at 30° and 37° in the presence or absence of a destabilizing P66L mutation in DHFR, as noted at top. All cells were grown in 96-well plates. Error bars, SD.

We next examined stability differences between wild-type and mutant versions of SMN1, associated with spinal muscular atrophy. In humans, two genes exist, *SMN1* and *SMN2*, and affected patients typically have a deletion in *SMN1*, but retain *SMN2* (Lefebvre *et al.* 1995). *SMN2* is nearly identical to *SMN1*, but has a base pair change that affects splicing of exon 7, resulting in a shorter, less stable gene product (SMNΔ7) (Lorson *et al.* 1999; Monani *et al.* 1999). Using IDESA, we examined yeast expressing wild-type SMN1 (dhSMN) or SMNΔ7 (Figure 5). While differences were subtle at 30°, at 37° yeast expressing dhSMNΔ7 showed distinctly reduced growth, correlating with the reduced stability of this variant.

Based on the results with wild-type and disease alleles, we predicted that IDESA would be useful for engineering temperature-sensitive alleles for conditional loss-of-function studies. Standard methods for identification of temperature-sensitive alleles are based on *in vivo* genetic screens, functional tests, or approaches such as Western blotting that are not amenable to selection. We tested two variants of p53, one (A138V) that shows a temperature-sensitive phenotype in human and mouse models (Hirano *et al.* 1995) and another (Y220C) that is a destabilizing mutation found in human cancers (Joerger *et al.* 2006). Yeast expressing the temperature-sensitive or disease variants exhibited reduced growth at both 30° and 37° compared to yeast expressing wild type p53 (dhp53) (Figure 5). In contrast to a previously described activity-based p53 assay in yeast (Ishioka *et al.* 1993), IDESA is independent of the biological activity of p53 and the reduced growth reflects only a change in stability of the protein. Since large numbers of mutants can be generated and screened rapidly in yeast, we expect that IDESA will be useful in screens to identify novel temperature-sensitive alleles.

Chemical screens for stabilizing molecules using IDESA

One area of promise in medicine is the use of pharmacological chaperones, small molecules that rescue misfolded disease variants. Destabilized proteins often retain the ability to function at a low level, but may be degraded by the cell's quality control machinery or localized to an incorrect cellular compartment. For mutants that retain function but are present at low levels, addition of stabilizing molecules may help to alleviate the disease phenotype. Identifying such molecules require high-throughput assays for activity or stability to screen large chemical libraries. In constrast to inhibitory compounds, stabilizing compounds often have more subtle effects (slightly increasing the steady-state levels of a protein, for example), and thus any high-throughput assay designed to identify such compounds must be highly sensitive and reproducible.

Based on our initial findings that IDESA reproducibly reports subtle changes in protein levels within cells, we hypothesized that this assay would be sufficiently sensitive to allow identification of stabilizing molecules. Unlike other sensitive approaches such as Western blotting, IDESA is well suited for high-throughput screening. We thus tested a high-throughput version of the assay in 96-well plates, using methodology that should be effective for screening tens of thousands of compounds, and screened a 1200-member Sigma LOPAC library for compounds that stabilize P66LdhDJ1^{L166P}. We expected that compounds that stabilized the DHFR fusion protein would increase DHFR levels, resulting in a net increase in yeast growth. In duplicate screens, three compounds, aminopterin, methotrexate, and trimethoprim, increased growth of yeast. Counterintuitively, these compounds are all competitive inhibitors of DHFR. However, while they inhibit DHFR activity, they also significantly stabilize the enzyme (Sasso *et al.* 1995; Levy *et al.* 1999). We speculated that at the subinhibitory concentrations used in screening, the inhibitors were acting as pharmacological chaperones, giving a net increase in functional DHFR enzyme and a corresponding increase in growth of yeast. We carried out titrations of one of the inhibitors, methotrexate, using IDESA constructs P66LdhDJ1, P66LdhDJ1^{L166P}, and P66LdhSOD^{G37R}. Although methotrexate is a strong inhibitor of mammalian DHFR [K_i ~12.9 pM for mouse DHFR (Dicker *et al.* 1993)], yeast expressing P66LdhDJ1, P66LdhDJ1^{L166P}, and P66LdhSOD^{G37R} showed an increase in growth with methotrexate that was maximal at 1 μM (1.6- to 3.8-fold increase in growth over nontreated cells) and that declined at higher concentrations (Figure 6A). Increased growth accompanied a corresponding increase in protein levels: expression of P66LdhSOD^{G37R} was increased 2.5- to 3-fold with 1 μM or 10 μM methotrexate, indicating significant ligand-induced stabilization (Figure 6B). Since the DHFR inhibitors affected both dhSOD and dhDJ1, they presumably bind DHFR and not the target proteins. Although the identified compounds appear to stabilize DHFR and not the target protein, they act in a similar way to a ligand that would stabilize the target protein, increasing levels of the DHFR fusion. Thus, this work establishes that IDESA is sufficiently sensitive to identify stabilizing compounds that increase the steady-state levels of the DHFR fusion protein. Clearly, compounds that bind DHFR will be false-positive hits with this screen. However, we expect their abundance in an unbiased library to be much lower than in the Sigma LOPAC library (4%), and a variety of straightforward approaches such as differential scanning fluorimetry (Niesen *et al.* 2007) exist that can be used to eliminate DHFR-binding compounds in secondary screens.

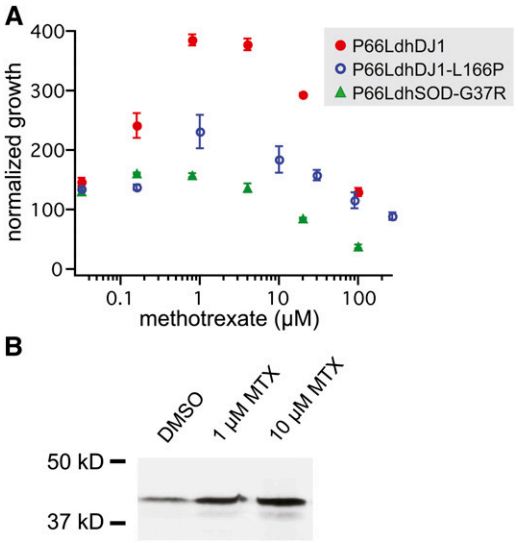

Figure 6 Methotrexate is a pharmacological chaperone for P66LdhSOD^{G37R}. (A) pTB3 plasmids expressing P66LdhDJ1, P66LdhDJ1^{L166P}, and P66LdhSOD^{G37R} were expressed in TH5 cells and incubated with indicated concentrations of methotrexate. Growth was monitored in 96-well plates for 48 hr at 37° (for P66LdhSOD^{G37R}) or at 30° (for P66LdhDJ1 and P66LdhDJ1^{L166P}). The normalized data are expressed as a percentage of growth in the absence of methotrexate. Error bars, SD. (B) Levels of P66LdhSOD^{G37R} are increased in the presence of methotrexate. Shown is an immunoblot of soluble HA-tagged P66LdhSOD^{G37R} protein expressed using a galactose-inducible promoter in strain W303-1A. Samples were induced in the presence of DMSO, 1 μM methotrexate (MTX), or 10 μM MTX.

Discussion

The IDESA platform provides a generalizable *in vivo* assay that accurately couples protein steady-state levels to cell proliferation in eukaryotes. The design of the assay, which is tunable using temperature and/or mutations to decrease DHFR activity to threshold levels for yeast survival, provides remarkable sensitivity. Thus, by optimizing and tuning the assay for specific proteins, small differences in protein levels can be observed as robust changes in growth. In studies characterizing the stability of disease variants, we demonstrate that proteins that have reduced thermodynamic stabilities tend to grow more poorly in IDESA, but other properties related to *in vivo* expression, such as protein

half-lives and the tendency of a protein to aggregate, also affect protein steady-state levels and corresponding yeast growth. Ultimately, the assay offers an accurate and sensitive measure of protein steady-state levels that would be comparable to measurements obtained by Western blotting. However, unlike Western blotting, IDESA is amenable to high-throughput analysis. Thus, this assay can be used in large screens to identify factors that enhance the stability of target proteins, to examine the consequences of amino acid changes on protein stability or to find temperature-sensitive alleles for proteins of interest.

Using the primary hyperoxaluria-associated protein AGT, we demonstrate use of IDESA in profiling the stability of mutant alleles. Integration of stability phenotypes with activity profiles reveals clusters of mutations that would not be found using activity profiles alone. In our studies, we identified a cluster of three mutants found in PH1 patients that showed normal growth in the IDESA assay but that had greatly reduced enzyme activity. The mutations are distal from the protein active site but cluster together within the tertiary protein structure. Molecular dynamics simulations of one of the mutants indicated perturbation of cofactor binding at the active site. We speculate that even subtle changes in this region of the protein may have consequential effects on cofactor binding and enzyme activity and are currently carrying out a detailed biochemical analysis of the molecular defects resulting from these changes.

Based on the high sensitivity and reproducibility of IDESA and the ease of use in a high-throughput format, we examined the utility of the assay in screening for pharmacological chaperones (stabilizing compounds). Although a number of other approaches for high-throughput screening for stabilizing compounds using *in vitro* purified protein exist, many proteins are difficult to purify, and few generalizable assays exist for screening proteins *in vivo*. We performed a small high-throughput compound library screen with IDESA using a Parkinson's disease-related variant of DJ-1 and identified three DHFR inhibitors as hits. At subinhibitory concentrations, these compounds appear to act as pharmacological chaperones for DHFR, stabilizing the protein and allowing increased levels of the DHFR reporter to accumulate. Although we did not identify compounds that specifically stabilized the DJ-1 portion of the molecule, these results show that stabilizing molecules that increase levels of the DHFR fusion protein can be identified by using IDESA to monitor subtle increases in yeast growth, and we anticipate that much larger screens may allow identification of compounds that stabilize specific target proteins.

While all of the target inserts tested here comprised entire proteins, we expect that domains of proteins can also be tested, extending this approach to use with domains of membrane proteins. Although this assay was developed in yeast, we also expect that it should be transferable to mammalian cells, using either commonly available DHFR knockout lines or methotrexate resistant mutations in the reporter. Finally, we expect IDESA to be useful not only in screens for therapeutic chemical chaperones, but also for identifying genetic modifiers of protein stability in combination with shRNA or other genome-wide loss- or gain-of-function tools. Using approaches such as described here, IDESA should provide a powerful platform for characterization of a variety of genetic mutations.

Acknowledgments

We thank Chris Danpure (University College London) for providing an antibody to human AGT, Elliot Androphy (U. Mass Medical School) for providing cDNA containing SMN1, Tso-Pang Yao (Duke University) for providing cDNA containing p53, and Peter Quail (UC Berkeley) for providing the plasmids PhyB(NT)-GBD and PIF3-GAD. This work was supported by grants from the National Institutes of Health National Institute of Diabetes and Digestive and Kidney Diseases (NIDDK) (grant numbers R01DK81584, R21DK075291) and the Oxalosis and Hyperoxaluria Foundation to C.L.T. and by the Italian Telethon Foundation (GGP 10092).

Literature Cited

Belle, A., A. Tanay, L. Bitincka, R. Shamir, and E. K. O'Shea, 2006 Quantification of protein half-lives in the budding yeast proteome. Proc. Natl. Acad. Sci. USA 103: 13004–13009.

Blackinton, J., R. Ahmad, D. W. Miller, M. P. van der Brug, R. M. Canet-Aviles *et al.*, 2005 Effects of DJ-1 mutations and polymorphisms on protein stability and subcellular localization. Brain Res. Mol. Brain Res. 134: 76–83.

Cabantous, S., Y. Rogers, T. C. Terwilliger, and G. S. Waldo, 2008 New molecular reporters for rapid protein folding assays. PLoS ONE 3: e2387.

Cardoso, R. M., M. M. Thayer, M. DiDonato, T. P. Lo, C. K. Bruns *et al.*, 2002 Insights into Lou Gehrig's disease from the structure and instability of the A4V mutant of human Cu,Zn superoxide dismutase. J. Mol. Biol. 324: 247–256.

Cellini, B., M. Bertoldi, R. Montioli, A. Paiardini, and C. Borri Voltattorni, 2007 Human wild-type alanine:glyoxylate aminotransferase and its naturally occurring G82E variant: functional properties and physiological implications. Biochem. J. 408: 39–50.

Cellini, B., R. Montioli, S. Bianconi, J. P. Lopez-Alonso, and C. B. Voltattorni, 2008 Construction, purification and characterization of untagged human liver alanine-glyoxylate aminotransferase expressed in *Escherichia coli*. Protein Pept. Lett. 15: 153–159.

Cellini, B., A. Lorenzetto, R. Montioli, E. Oppici, and C. B. Voltattorni, 2010a Human liver peroxisomal alanine:glyoxylate aminotransferase: different stability under chemical stress of the major allele, the minor allele, and its pathogenic G170R variant. Biochimie 92: 1801–1811.

Cellini, B., R. Montioli, A. Paiardini, A. Lorenzetto, F. Maset *et al.*, 2010b Molecular defects of the glycine 41 variants of alanine glyoxylate aminotransferase associated with primary hyperoxaluria type I. Proc. Natl. Acad. Sci. USA 107: 2896–2901.

Cheng, S. H., R. J. Gregory, J. Marshall, S. Paul, D. W. Souza *et al.*, 1990 Defective intracellular transport and processing of CFTR is the molecular basis of most cystic fibrosis. Cell 63: 827–834.

Cooper, A. A., A. D. Gitler, A. Cashikar, C. M. Haynes, K. J. Hill *et al.*, 2006 Alpha-synuclein blocks ER-Golgi traffic and Rab1 rescues neuron loss in Parkinson's models. Science 313: 324–328.

Coulter-Mackie, M. B., and Q. Lian, 2006 Consequences of missense mutations for dimerization and turnover of alanine:glyoxylate aminotransferase: study of a spectrum of mutations. Mol. Genet. Metab. 89: 349–359.

Danpure, C. J., and P. R. Jennings, 1986 Peroxisomal alanine: glyoxylate aminotransferase deficiency in primary hyperoxaluria type I. FEBS Lett. 201: 20–24.

Dicker, A. P., M. C. Waltham, M. Volkenandt, B. I. Schweitzer, G. M. Otter *et al.*, 1993 Methotrexate resistance in an in vivo mouse tumor due to a non-active-site dihydrofolate reductase mutation. Proc. Natl. Acad. Sci. USA 90: 11797–11801.

Dohmen, R. J., P. Wu, and A. Varshavsky, 1994 Heat-inducible degron: a method for constructing temperature-sensitive mutants. Science 263: 1273–1276.

Ehrnhoefer, D. E., M. Duennwald, P. Markovic, J. L. Wacker, S. Engemann *et al.*, 2006 Green tea (-)-epigallocatechin-gallate modulates early events in huntingtin misfolding and reduces toxicity in Huntington's disease models. Hum. Mol. Genet. 15: 2743–2751.

Ercikan-Abali, E. A., S. Mineishi, Y. Tong, S. Nakahara, M. C. Waltham *et al.*, 1996 Active site-directed double mutants of dihydrofolate reductase. Cancer Res. 56: 4142–4145.

Foit, L., G. J. Morgan, M. J. Kern, L. R. Steimer, A. A. von Hacht *et al.*, 2009 Optimizing protein stability in vivo. Mol. Cell 36: 861–871.

Forman, H. J., and I. Fridovich, 1973 On the stability of bovine superoxide dismutase. The effects of metals. J. Biol. Chem. 248: 2645–2649.

Frishberg, Y., C. Rinat, A. Shalata, I. Khatib, S. Feinstein *et al.*, 2005 Intra-familial clinical heterogeneity: absence of genotype-phenotype correlation in primary hyperoxaluria type 1 in Israel. Am. J. Nephrol. 25: 269–275.

Furukawa, Y., and T. V. O'Halloran, 2005 Amyotrophic lateral sclerosis mutations have the greatest destabilizing effect on the apo- and reduced form of SOD1, leading to unfolding and oxidative aggregation. J. Biol. Chem. 280: 17266–17274.

Hirano, Y., K. Yamato, and N. Tsuchida, 1995 A temperature sensitive mutant of the human p53, Val138, arrests rat cell growth without induced expression of cip1/waf1/sdi1 after temperature shift-down. Oncogene 10: 1879–1885.

Hopper, E. D., A. M. Pittman, M. C. Fitzgerald, and C. L. Tucker, 2008 In vivo and in vitro examination of stability of primary hyperoxaluria-associated human alanine:glyoxylate aminotransferase. J. Biol. Chem. 283: 30493–30502.

Ishioka, C., T. Frebourg, Y. X. Yan, M. Vidal, S. H. Friend *et al.*, 1993 Screening patients for heterozygous p53 mutations using a functional assay in yeast. Nat. Genet. 5: 124–129.

Joerger, A. C., H. C. Ang, and A. R. Fersht, 2006 Structural basis for understanding oncogenic p53 mutations and designing rescue drugs. Proc. Natl. Acad. Sci. USA 103: 15056–15061.

Lefebvre, S., L. Burglen, S. Reboullet, O. Clermont, P. Burlet *et al.*, 1995 Identification and characterization of a spinal muscular atrophy-determining gene. Cell 80: 155–165.

Leinweber, B., E. Barofsky, D. F. Barofsky, V. Ermilov, K. Nylin *et al.*, 2004 Aggregation of ALS mutant superoxide dismutase expressed in *Escherichia coli*. Free Radic. Biol. Med. 36: 911–918.

Levy, F., J. A. Johnston, and A. Varshavsky, 1999 Analysis of a conditional degradation signal in yeast and mammalian cells. Eur. J. Biochem. 259: 244–252.

Lindberg, M. J., R. Bystrom, N. Boknas, P. M. Andersen, and M. Oliveberg, 2005 Systematically perturbed folding patterns of amyotrophic lateral sclerosis (ALS)-associated SOD1 mutants. Proc. Natl. Acad. Sci. USA 102: 9754–9759.

Lorson, C. L., E. Hahnen, E. J. Androphy, and B. Wirth, 1999 A single nucleotide in the SMN gene regulates splicing and is responsible for spinal muscular atrophy. Proc. Natl. Acad. Sci. USA 96: 6307–6311.

Lumb, M. J., and C. J. Danpure, 2000 Functional synergism between the most common polymorphism in human alanine: glyoxylate aminotransferase and four of the most common disease-causing mutations. J. Biol. Chem. 275: 36415–36422.

Lumb, M. J., G. M. Birdsey, and C. J. Danpure, 2003 Correction of an enzyme trafficking defect in hereditary kidney stone disease in vitro. Biochem. J. 374: 79–87.

Malgieri, G., and D. Eliezer, 2008 Structural effects of Parkinson's disease linked DJ-1 mutations. Protein Sci. 17: 855–868.

Monani, U. R., C. L. Lorson, D. W. Parsons, T. W. Prior, E. J. Androphy *et al.*, 1999 A single nucleotide difference that alters splicing patterns distinguishes the SMA gene SMN1 from the copy gene SMN2. Hum. Mol. Genet. 8: 1177–1183.

Mu, T. W., D. S. Ong, Y. J. Wang, W. E. Balch, J. R. Yates 3rd. *et al.*, 2008 Chemical and biological approaches synergize to ameliorate protein-folding diseases. Cell 134: 769–781.

Neef, D. W., M. L. Turski, and D. J. Thiele, 2010 Modulation of heat shock transcription factor 1 as a therapeutic target for small molecule intervention in neurodegenerative disease. PLoS Biol. 8: e1000291.

Niesen, F. H., H. Berglund, and M. Vedadi, 2007 The use of differential scanning fluorimetry to detect ligand interactions that promote protein stability. Nat. Protoc. 2: 2212–2221.

Oppici, E., R. Montioli, A. Lorenzetto, S. Bianconi, C. Borri Voltattorni *et al.*, 2012 Biochemical analyses are instrumental in identifying the impact of mutations on holo and/or apo-forms and on the region(s) of alanine:glyoxylate aminotransferase variants associated with primary hyperoxaluria type I. Mol. Genet. Metab. 105: 132–140.

Pace, C. N., B. A. Shirley, and J. T. Thompson, 1989 *Measuring the Conformational Stability of a Protein*. IRL Press, Oxford.

Parsell, D. A., and R. T. Sauer, 1989 The structural stability of a protein is an important determinant of its proteolytic susceptibility in *Escherichia coli*. J. Biol. Chem. 264: 7590–7595.

Pedemonte, N., G. L. Lukacs, K. Du, E. Caci, O. Zegarra-Moran *et al.*, 2005 Small-molecule correctors of defective DeltaF508-CFTR cellular processing identified by high-throughput screening. J. Clin. Invest. 115: 2564–2571.

Purdue, P. E., Y. Takada, and C. J. Danpure, 1990 Identification of mutations associated with peroxisome-to-mitochondrion mistargeting of alanine/glyoxylate aminotransferase in primary hyperoxaluria type 1. J. Cell Biol. 111: 2341–2351.

Sali, A., and T. L. Blundell, 1993 Comparative protein modelling by satisfaction of spatial restraints. J. Mol. Biol. 234: 779–815.

Sasso, S., I. Protasevich, R. Gilli, A. Makarov, and C. Briand, 1995 Thermal denaturation of bacterial and bovine dihydrofolate reductases and their complexes with NADPH, trimethoprim and methotrexate. J. Biomol. Struct. Dyn. 12: 1023–1032.

Shaw, B. F., and J. S. Valentine, 2007 How do ALS-associated mutations in superoxide dismutase 1 promote aggregation of the protein? Trends Biochem. Sci. 32: 78–85.

Shimizu-Sato, S., E. Huq, J. M. Tepperman, and P. H. Quail, 2002 A light-switchable gene promoter system. Nat. Biotechnol. 20: 1041–1044.

Stathopulos, P. B., J. A. Rumfeldt, G. A. Scholz, R. A. Irani, H. E. Frey *et al.*, 2003 Cu/Zn superoxide dismutase mutants associated with amyotrophic lateral sclerosis show enhanced formation of aggregates in vitro. Proc. Natl. Acad. Sci. USA 100: 7021–7026.

Su, L. J., P. K. Auluck, T. F. Outeiro, E. Yeger-Lotem, J. A. Kritzer *et al.*, 2010 Compounds from an unbiased chemical screen reverse both ER-to-Golgi trafficking defects and mitochondrial

dysfunction in Parkinson's disease models. Dis. Model Mech. 3: 194–208.
Sussman, J. L., D. Lin, J. Jiang, N. O. Manning, J. Prilusky *et al.*, 1998 Protein Data Bank (PDB): database of three-dimensional structural information of biological macromolecules. Acta Crystallogr. D Biol. Crystallogr. 54: 1078–1084.
Tarassov, K., V. Messier, C. R. Landry, S. Radinovic, M. M. Serna Molina *et al.*, 2008 An in vivo map of the yeast protein interactome. Science 320: 1465–1470.
Tucker, C. L., and S. Fields, 2001 A yeast sensor of ligand binding. Nat. Biotechnol. 19: 1042–1046.
Van Der Spoel, D., E. Lindahl, B. Hess, G. Groenhof, A. E. Mark *et al.*, 2005 GROMACS: fast, flexible, and free. J. Comput. Chem. 26: 1701–1718.
Waldo, G. S., B. M. Standish, J. Berendzen, and T. C. Terwilliger, 1999 Rapid protein-folding assay using green fluorescent protein. Nat. Biotechnol. 17: 691–695.
Wigley, W. C., R. D. Stidham, N. M. Smith, J. F. Hunt, and P. J. Thomas, 2001 Protein solubility and folding monitored in vivo by structural complementation of a genetic marker protein. Nat. Biotechnol. 19: 131–136.
Williams, E. L., C. Acquaviva, A. Amoroso, F. Chevalier, M. Coulter-Mackie *et al.*, 2009 Primary hyperoxaluria type 1: update and additional mutation analysis of the AGXT gene. Hum. Mutat. 30: 910–917.
Yam, G. H., C. Zuber, and J. Roth, 2005 A synthetic chaperone corrects the trafficking defect and disease phenotype in a protein misfolding disorder. FASEB J. 19: 12–18.
Zhang, X., S. M. Roe, Y. Hou, M. Bartlam, Z. Rao *et al.*, 2003 Crystal structure of alanine:glyoxylate aminotransferase and the relationship between genotype and enzymatic phenotype in primary hyperoxaluria type 1. J. Mol. Biol. 331: 643–652.

Communicating editor: C. Boone